Near-surface Stratification Due to Ice Melt Biases Arctic Air-Sea CO_2 Flux Estimates

Yuanxu Dong[1,2], Mingxi Yang[2], Dorothee C. E. Bakker[1], Peter S. Liss[1], Vassilis Kitidis[2], Ian Brown[2], Melissa Chierici[3,4], Agneta Fransson[5] and Thomas G. Bell[2]

[1]Centre for Ocean and Atmospheric Sciences, School of Environmental Sciences, University of East Anglia, Norwich, UK

[2]Plymouth Marine Laboratory, Prospect Place, Plymouth, UK

[3]Institute of Marine Research, Fram Centre, Tromsø, Norway

[4]Department of Arctic Geophysics, University Centre in Svalbard, Longyearbyen, Norway

[5]Norwegian Polar Institute, Fram Centre, Tromsø, Norway

Correspondence to: Yuanxu Dong (Yuanxu.Dong@uea.ac.uk)

Key points:

- Seawater CO_2 fugacity ($f\mathrm{CO}_{2w}$) vertical gradients are generated by fresh and cold sea-ice melt water, which lowers surface $f\mathrm{CO}_{2w}$
- Air-sea CO_2 fluxes are biased when estimated using $f\mathrm{CO}_{2w}$ observations from the sub-surface (6 m depth) in sea-ice melt areas
- Summertime sea-ice melt could result in a 6–17% (with high uncertainty) underestimate of annual Arctic Ocean CO_2 uptake

Abstract Air-sea carbon dioxide (CO_2) flux is generally estimated by the bulk method using upper ocean CO_2 fugacity measurements. In the summertime Arctic, sea-ice melt results in stratification within the upper ocean (top ~10 m), which can bias bulk CO_2 flux estimates when the seawater CO_2 fugacity is taken from a ship's seawater inlet at ~6 m depth (fCO_{2w_bulk}). Direct flux measurements by eddy covariance are unaffected by near-surface stratification. We use eddy covariance CO_2 flux measurements to infer sea surface CO_2 fugacity ($fCO_{2w\_surface}$) in the Arctic Ocean. In sea-ice melt regions, $fCO_{2w\_surface}$ values are consistently lower than fCO_{2w_bulk} by an average of 39 µatm. Lower $fCO_{2w\_surface}$ can be partially accounted for by fresher (≥ 27%) and colder (17%) melt waters. A back-of-the-envelope calculation shows that neglecting the summertime sea-ice melt could lead to a 6–17% underestimate of the annual Arctic Ocean CO_2 uptake.

Plain language summary The Arctic Ocean is considered to be a strong sink for atmospheric CO_2. The air-sea CO_2 flux is almost always estimated indirectly using bulk seawater CO_2 fugacity measured from the ship's seawater inlet at typically ~6 m depth. However, sea-ice melt results in near-surface stratification and can cause a bias in air-sea CO_2 flux estimates if the bulk water CO_2 fugacity is used. The micrometeorological eddy covariance flux technique is not affected by stratification. Here for the first time, we employ eddy covariance measurements to assess the impact of sea-ice melt on Arctic Ocean CO_2 uptake estimates. The results show that the summertime near-surface stratification due to sea-ice melt could lead to an ~10% (with high uncertainty) underestimation of the annual Arctic Ocean CO_2 uptake.

1. Introduction

The Arctic Ocean is a strong sink of atmospheric CO_2 due to the active biological production and high CO_2 solubility in cold waters (Anderson et al., 1998; Takahashi et al., 2009). While only accounting for 4% of the world ocean by area and seasonally covered by sea ice, the Arctic Ocean contributes 5–14% (66–199 Tg C yr^{-1}, Bates & Mathis, 2009; Yasunaka et al., 2018) of mean global atmospheric CO_2 removal every year (~1400 Tg C yr^{-1}, Takahashi et al., 2009; Landschützer et al., 2014). However, this Arctic carbon sink is rapidly changing due to climate change. The Arctic warming rate has been more than twice as fast as the global average over the past 5 decades (Romanovsky et al., 2017). The sea-ice extent in the Arctic Ocean in September decreased at a rate of 13.1% $decade^{-1}$ during 1979–2020 relative to the 1981–2010 average (Perovich et al., 2020). Sea-ice loss reinforces upper ocean warming due to reduced surface albedo and increased shortwave penetration, which in turn inhibits sea-ice formation in winter and allows for acceleration of summertime sea-ice loss (Perovich et al., 2007). The reduction in sea-ice coverage in polar regions is expected to increase CO_2 uptake due to larger sea-ice free area, longer sea-ice free period, more freshwater at the surface and greater biological primary production (Bates & Mathis, 2009; Arrigo & van Dijken, 2015; McPhee et al., 2009; Perovich et al., 2020).However, sea-ice melt also causes near-surface stratification and suppresses water mixing between the surface and sub-surface, which likely generates upper-ocean gradients in temperature, salinity, dissolved inorganic carbon (DIC), total alkalinity (TA) and thus seawater CO_2 fugacity (Rysgaard et al., 2007; Li et al., 2009; Yamamoto-Kawai et al., 2009; Fransson et al., 2009, 2013; Cai et al., 2010; Else et al., 2013; Calleja et al., 2013; Miller et al., 2019; Ahmed et al., 2020).

The air-sea CO_2 flux (F_{CO_2}, mmol m^{-2} day^{-1}) is generally estimated indirectly by the bulk equation as the product of the gas transfer velocity and the air-sea gas concentration difference. Accounting for near-surface temperature gradients, Woolf et al. (2016) recommended:

$$F_{CO_2} = K_{660}(Sc/660)^{-0.5}\left(\alpha_{ss} f\mathrm{CO}_{2\mathrm{w}} - \alpha_s f\mathrm{CO}_{2\mathrm{a}}\right) \tag{1}$$

where K_{660} (cm h^{-1}) is the gas transfer velocity at a Schmidt number (Sc) of 660 (Wanninkhof et al., 2009). K_{660} is usually parameterized as a function of wind speed (e.g. Nightingale et al., 2000). α_{ss} and α_s are the CO_2 solubility (mol L^{-1} atm^{-1}, Weiss, 1974) in the subskin and skin seawater, respectively (Woolf et al., 2016). $f\mathrm{CO}_{2\mathrm{w}}$ and $f\mathrm{CO}_{2\mathrm{a}}$ are the CO_2 fugacity (µatm) near the sea surface and in the overlying atmosphere, respectively. Similarly, the air-sea sensible heat flux can be estimated by the bulk method using a parameterized sensible heat transfer velocity and the sea-air temperature difference (Text S1).

Air-sea exchange of sparingly soluble gases (e.g. CO_2) is limited mostly by transport within the waterside molecular diffusive layer (MDL, 20–200 µm depth; Jähne, 2009) just beneath the water surface (Liss & Slater, 1974). Thus, $f\mathrm{CO}_{2\mathrm{w}}$ represents the CO_2 fugacity at the base of MDL ($f\mathrm{CO}_{2\mathrm{w\_surface}}$). In practice, $f\mathrm{CO}_{2\mathrm{w}}$ measurements are generally made on bulk seawater from the ship's underway inlet (~6 m depth, $f\mathrm{CO}_{2\mathrm{w\_bulk}}$). For convenience, the upper several meters of the ocean are assumed to be homogeneous in bulk flux calculations (i.e. $f\mathrm{CO}_{2\mathrm{w}} = f\mathrm{CO}_{2\mathrm{w\_surface}} = f\mathrm{CO}_{2\mathrm{w\_bulk}}$).

However, incidences of near-surface stratification call into question the vertical homogeneity assumption. In the Arctic, three sea-ice related mechanisms likely drive near-surface vertical gradients in CO_2: 1) Brine drainage. When sea ice forms, carbonate species and salt are ejected into the water under the sea ice as part of brine drainage (e.g. Fransson et al., 2013), which depletes the CO_2 within the sea ice. The salty, dense water sinks and is eventually sequestered in the deep ocean (Rudels et al., 2005). 2) Surface photosynthesis. Phytoplankton are often found in the bottom ice or beneath the Arctic sea ice and their photosynthetic activity further reduces the CO_2 concentration within the sea ice (Assmy et al., 2017; Fransson et al., 2013, 2017). 3) Ikaite dissolution. Dissolution of sea-ice derived ikaite will consume CO_2 in Arctic surface waters (Fransson et al., 2017; Chierici et al., 2019). The latest measurements in the Arctic coastal waters show significant vertical fCO_{2w} gradients in the upper ocean (Ahmed et al., 2020; Miller et al., 2019). Miller et al. (2019) show both positive and negative fCO_{2w} gradients without separating the contributions of sea-ice melt and river runoff. Ahmed et al. (2020) show consistently negative gradients (i.e., $fCO_{2w\_surface} < fCO_{2w\ bulk}$) in the sea-ice melt regions. Vertical gradients, if left unaccounted for, will result in a bias in bulk air-sea CO_2 flux estimates.

The micrometeorological eddy covariance (EC) method derives CO_2 fluxes directly and represents an alternative approach for understanding Arctic air-sea CO_2 exchange. EC does not rely on seawater measurements (Text S2), and thus EC fluxes are not affected by near-surface vertical variation in seawater properties. However, polar oceans are a hostile environment and reliable direct CO_2 flux measurements by EC are scarce (Butterworth & Miller, 2016; Prytherch et al., 2017; Butterworth & Else, 2018; Prytherch & Yelland, 2021). This paper presents EC CO_2 and sensible heat flux data from two Changing Arctic Ocean Programme cruises. Directly measured fluxes were used to compute the implied sea surface fCO_{2w} and water temperature ($fCO_{2w\_surface}$, $T_{w\_surface}$). Comparisons of implied surface values with bulk measurements enable us to assess the impact of vertical gradients on bulk air-sea CO_2 flux estimates. We further speculate on the influence of near-surface stratification on bulk air-sea CO_2 flux estimates for the entire Arctic Ocean.

2. Methods

2.1 Description of Cruises

Cruise tracks of JR18006 and JR18007 (on RRS *James Clark Ross*, *JCR*)) and FS2019 (on RV *Kronprins Haakon*) are shown in Figure S1. JR18006 visited the Barents Sea between 28 June and 1 August 2019. JR18007 targeted the Fram Strait region within the Greenland Sea between

4 and 30 August 2019. DIC and TA were not measured during JR18006 and JR18007. Measurements taken between 2 and 5 September 2019 (between 0°W and 10°W) on cruise FS2019 were used to constrain the upper ocean carbonate system. Methods for DIC and TA measurements can be found in Chierici et al. (2019). The EC system on *JCR*, processing and quality control of fluxes, underway measurements and the meteorological observations are detailed elsewhere (Dong et al., 2021) and are briefly described in the supporting information (Text S3). fCO_{2w} measurements were only available during ice-free periods of JR18007.

2.2 Implied Surface Variables From Eddy Covariance Fluxes

We use Brunt–Väisälä frequency (N^2) threshold to identify stratified waters. N^2 at ~6 m depth is calculated from the CTD (conductivity, temperature, depth) profiles ($N^2 = -g(\rho_{7m} - \rho_{5m})/(2 * \rho_{7m})$ with gravitational acceleration g and seawater density ρ). Fischer et al. (2019) used $N^2 \geq 10^{-4}$ s^{-2} in upwelling waters, but we expect the threshold for near-surface stratification to be more evident in regions with sea- ice melt, so use a more robust threshold of $N^2 \geq 10^{-3}$ s^{-2}. Measurements in waters without a CTD cast and salinity below 34.5 are marked as having an 'unknown' stratification status.

The derivations of EC air-sea CO_2 flux (FCO_{2_EC}) and sensible heat flux (H_{S_EC}) are detailed in the supporting information (Text S2). The gas transfer velocity (hourly) is computed by replacing the bulk flux with the hourly EC flux in a rearrangement of Equation 1:

$$K_{660} = \frac{F_{\mathrm{CO_2\_EC}}}{(Sc/660)^{-0.5}\left(\alpha_{ss} f\mathrm{CO}_{2\mathrm{w\_bulk}} - \alpha_s f\mathrm{CO}_{2\mathrm{a}}\right)} \tag{2}$$

In regions with near-surface stratification, fCO_{2w_bulk} may not be representative of the surface (i.e. $fCO_{2w\_bulk} \neq fCO_{2w\_surface}$). Therefore, to derive a wind speed (U_{10N}) dependent parametrization of K_{660} from this project (K_{660_u}), only data from non-stratified waters are considered. K_{660_u} and the EC CO_2 flux observations are then used to compute the implied $fCO_{2w\_surface}$ for all water types (non-stratified and stratified):

$$f\mathrm{CO}_{2\mathrm{w\_surface}} = \frac{F_{\mathrm{CO_2\_EC}}}{K_{660\_\mathrm{u}}(Sc/660)^{-0.5}\,\alpha_{ss}} + \frac{\alpha_s}{\alpha_{ss}} f\mathrm{CO}_{2\mathrm{a}} \tag{3}$$

A similar approach is used to derive sensible heat transfer velocity (K_H) and compute the implied surface seawater temperature ($T_{w\_surface}$):

$$K_{\mathrm{H}} = \frac{H_{\mathrm{S\_EC}}}{\rho_{\mathrm{a}} c_{\mathrm{pa}}\left(T_{\mathrm{w\_bulk}} - \mathrm{d}T - T_{\mathrm{a}}\right)} \tag{4}$$

$$T_{\mathrm{w\_surface}} = \frac{H_{\mathrm{S\_EC}}}{\rho_{\mathrm{a}} c_{\mathrm{pa}} K_{\mathrm{H\_u}}} + T_{\mathrm{a}} \tag{5}$$

where K_H (cm h^{-1}) is parametrized with U_{10N} (K_{H_u}) using data from non-stratified waters (Figure S2). Here, ρ_a (kg m^{-3}) is the mean density of dry air, c_{pa} (J kg^{-1} K^{-1}) is the heat capacity of air and T_a (K) is the air temperature. The temperature offset due to the cool skin effect, dT (K), is estimated using the COARE 3.5 model (Edson et al., 2013; Fairall et al., 1996).

3. Results and discussion

3.1 CO_2 flux time series

The time series of hourly averaged EC and bulk fluxes for CO_2 and heat are shown for cruise JR18007 (Figure 1). The bulk CO_2 flux is calculated from fCO_{2w_bulk}, fCO_{2a} and T_{w_bulk} measurements using the gas transfer velocity parametrisation from Nightingale et al. (2000). The bulk sensible heat flux is computed using the COARE 3.5 model (Edson et al., 2013). The sea ice concentration (Figure 1d) is derived from the Advanced Microwave Scanning Radiometer-Earth Observing System (AMSR-E, daily and 3.125 km resolution; Spreen et al., 2008).

Stratified areas were located at the edge of or within the sea ice (Figure S1), with relatively low near-surface salinity and temperature (Figure 1) suggesting that sea-ice melt is the principal reason for near-surface stratification. Terrestrial runoff as a source of freshwater is unlikely because the ship was far from land (> 50 km) in the stratified stations (Figure S1). Furthermore, there were no significant precipitation events during the cruise, ruling out surface freshening due to precipitation.

The relatively good agreement between EC fluxes and bulk air-sea CO_2 fluxes in non-stratified regions (Figure 1a and S3) suggests that the data (EC fluxes and underway fCO_{2w_bulk}) are reliable and that the Nightingale et al. (2000) gas transfer velocity parameterization is reasonable for this study region. In areas with near-surface stratification (stations 6 and 16), bulk CO_2 fluxes are consistently less negative (lower in magnitude) than EC CO_2 fluxes (Figure 1a). Meanwhile, bulk sensible heat fluxes are slightly higher than EC fluxes in stratified regions.

Another intriguing feature is that EC sensible heat fluxes were close to zero during sea ice stations 8 and 9, but EC CO_2 fluxes were still significant. The sea ice concentration data (Figure 1d) show that the sea surface was not fully ice-covered in this region. One possible reason for near-zero sensible heat flux but detectable CO_2 flux is that the surface (seawater or sea ice) temperature was close to the air temperature, while an fCO_2 gradient existed across the sea surface. Also, air-sea CO_2 exchange is mainly controlled by waterside processes (Liss & Slater, 1974), whereas the air-sea heat exchange is controlled by airside processes (Yang et al., 2016). It is possible that the impact of sea ice on waterside controlled gases (e.g. CO_2) is different to the impact on airside controlled gases and heat.

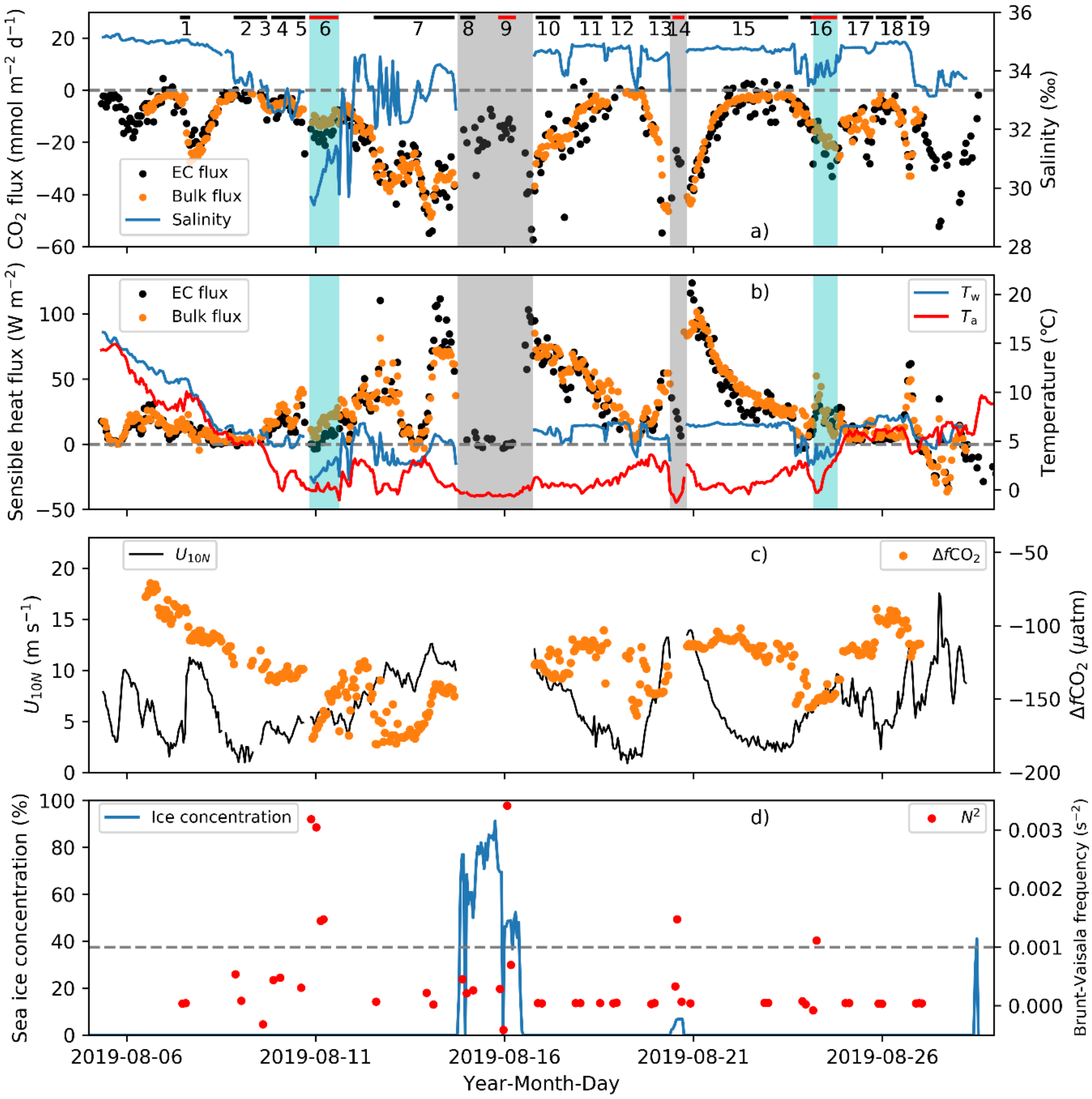

Figure 1. Time series of hourly fluxes and environmental variables on JR18007. Negative (positive) fluxes represent ocean sinks (sources): a) EC and bulk air-sea CO_2 fluxes, and salinity at 6 m depth. Light blue shading shows near-surface stratification (identified from CTD profiles). Grey shading indicates ice-covered waters where the underway seawater system was shut off. Dashes on the top axis correspond to CTD stations. Stations with near-surface stratification are in red. Dash length represents

the duration on station; b) EC and bulk sensible heat flux, seawater temperature (T_w) at 6 m depth and air temperature (T_a); c) 10-m neutral wind speed and air-sea CO_2 fugacity difference ($\Delta fCO_2 = fCO_{2w\_bulk} - fCO_{2a}$); d) Sea ice concentration (Spreen et al., 2008) and Brunt–Väisälä frequency (N^2) at 6 m depth.

3.2 Gas Transfer Velocity

Dong et al. (2021) show that the hourly EC air-sea CO_2 flux relative uncertainty is ~20% on average during JR18007. The ΔfCO_2 (= $fCO_{2w\_bulk} - fCO_{2a}$) ranges from -181 to -71 µatm (-130 µatm on average, Figure 1c) during JR18007. The relatively low flux uncertainty and large ΔfCO_2 values enable us to estimate the gas transfer velocity (K_{660}) with high accuracy. Figure 2 shows K_{660} derived from quality-controlled EC CO_2 fluxes and ΔfCO_2 observations, plotted against 10-m neutral wind speed (U_{10N}); the latter is determined from measurements of wind speed adjusted to U_{10N} using the COARE 3.5 model (Edson et al., 2013). There are 298 hourly averaged K_{660} values. 239 hourly K_{660} values from non-stratified waters are binned in wind speed intervals of 1 m s^{-1} and the bin averages (red squares) are used to derive a least square quadratic fit. The fit ($K_{660\_u} = 0.220\ U_{10N}^2 + 2.213$) agrees fairly well with a widely-used K_{660} parameterization based on dual tracer results (Nightingale et al., 2000) and a more recent parameterization derived from EC air-sea CO_2 flux measurements (Butterworth & Miller, 2016).

The K_{660} data in stratified waters (21 hourly K_{660}) are consistently higher than the parameterized K_{660_u} curve. Including data from stratified waters and waters with unknown stratification status (38 hourly K_{660}) decreases the strength of the quadratic fit between hourly K_{660} and U_{10N} from $R^2 = 0.801$ to $R^2 = 0.777$ (Table S1). This is most likely due to a vertical gradient in fCO_{2w}, where fCO_{2w_bulk} systematically exceeds $fCO_{2w\_surface}$ (see Section 3.3).

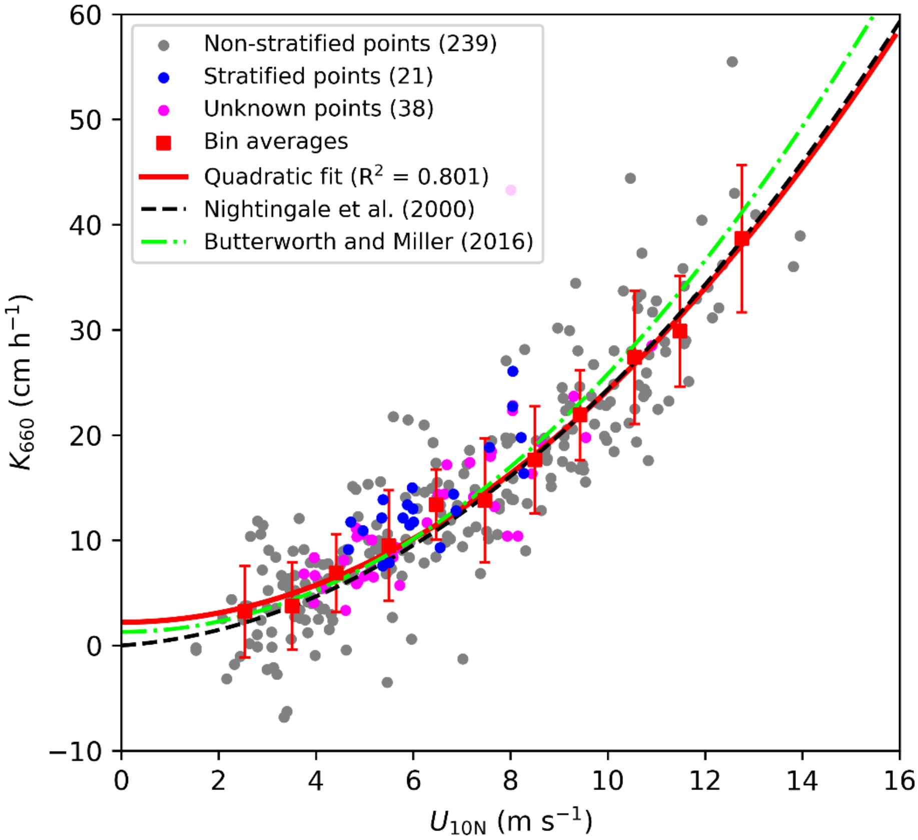

Figure 2. Relationship between the CO_2 gas transfer velocity (K_{660}, derived from hourly EC air-sea CO_2 flux measurements) and wind speed (U_{10N}) during JR18007. Grey dots represent K_{660} in non-stratified waters, blue dots correspond to K_{660} in stratified waters, and magenta dots indicate data with unknown stratification status. Red squares are 1 m s^{-1} bin averages of the non-stratified values, with error bars representing 1 standard deviation. The red curve is a quadratic parameterization ($K_{660\_u} = 0.220\ U_{10N}^2 + 2.213$; $R^2 = 0.801$). The K_{660} parameterizations of Nightingale et al. (2000) (black dashed) and Butterworth & Miller (2016) (green dot dashed) are also shown.

3.3 Implied Sea Surface CO_2 Fugacity and Temperature

The K_{660} parameterization in Figure 2 and the K_H parameterizations (Figure S2) are used for estimating $fCO_{2w\_surface}$ (Equation 3) and $T_{w\_surface}$ (Equation 5). Data at low wind speeds (U_{10N} < 4 m s^{-1}) are excluded from these calculations because of the low signal-to-noise ratios of EC fluxes and larger relative uncertainties in transfer velocities during calm conditions (Dong et al., 2021).

Figure 3 shows the comparison between hourly averages of the bulk seawater measurements (fCO_{2w_bulk} and, in the case of temperature, adjusted for the cool skin: $T_w - dT$) and the implied surface values ($fCO_{2w\_surface}$ and $T_{w\_surface}$). In non-stratified waters (grey dots in Figure 3a), the means of the two fCO_{2w} values compare reasonably well, even though the $fCO_{2w\_surface}$ values have a larger range than fCO_{2w_bulk} due to variability in the EC CO_2 flux observations and the uncertainty in the K_{660} parameterization. In stratified waters (blue dots in Figure 3a), the implied $fCO_{2w\_surface}$ values are consistently lower than fCO_{2w_bulk}, indicating that bulk measurements are not representative of the surface. Similarly, EC implied $T_{w\_surface}$ values are consistently lower than the bulk water temperature in low salinity areas (≤ 32, Figure 3b). These data corroborate the CTD profiles from JR18007 (Figure S4) and suggest that the surface water is colder and fresher than bulk water in regions with sea-ice melt.

Within the stratified areas during JR18007, $fCO_{2w\_surface}$ (mean = 208 μatm) is on average 39 ± 39 μatm lower than fCO_{2w_bulk} (mean = 247 μatm), while $T_{w\_surface}$ is on average 0.7 ± 0.8 °C below $T_{w\_bulk} - dT$. A temperature change of 0.7 °C should reduce fCO_{2w} by 7 μatm according to the Takahashi et al. (1993) empirical temperature relationship (Equation S5), suggesting that the temperature effect accounts for 18% of the vertical fCO_{2w} gradient within the stratified area.

Although the top 4 m depth CTD data have been removed due to ship interferences and rough sea state, CTD profiles still indicate that seawater at 4 m depth is fresher than the 5–10 m water at the stratified stations (Figure S4). The shapes of near-surface salinity profiles generally mirror those of temperature profiles (i.e. the vertical salinity gradient is nearly the same as the temperature gradient in magnitude; Figure S4). Here we crudely assume that the salinity difference between the sea surface and 6 m depth is 0.7 (i.e. corresponding to the temperature difference of 0.7 °C). Variations in near-surface salinity alter carbonate chemistry and influence fCO_{2w}. We use bulk water (~6 m depth) DIC and TA measurements (Table S2) collected a month later from 9 stations in the nearby Fram Strait (Figure S1, the sea ice concentration had decreased from ~50% to ~0% during a previous week of the cruise) to estimate the influence of salinity change on the vertical fCO_{2w} gradient. The average DIC, TA and salinity were 1974 ± 19 μmol kg^{-1}, 2100 ± 22 μmol kg^{-1}, and 30.6 ± 0.6, respectively.

Bulk water DIC and TA are corrected to a sea surface salinity by dividing by bulk salinity and multiplying by surface salinity (= bulk salinity − 0.7). The calculated surface and measured bulk water DIC and TA are used to estimate the sensitivity in fCO_{2w} to salinity change (Lewis & Wallace, 1998; Van Heuven et al., 2011). We estimate that the vertical salinity gradient can explain a fCO_{2w} gradient of on average 10.6 ± 1.1 μatm. This salinity-related decrease in fCO_{2w} accounts for 27% of the near-surface vertical fCO_{2w} gradient. Considering that the surface seawater is expected to be rapidly warmed by solar radiation, whereas salinity is less affected by surface warming, the temperature effect will be more transitory than the salinity effect. Thus, the estimated salinity effect is likely conservative, i.e. greater than 27%.

Sea-ice-related plankton metabolism might be another reason for lower fCO_{2w} in the surface stratified layer. The CTD oxygen profiles show that the oxygen concentration increases close to the surface in the stratified stations (Figure S4). Chierici et al. (2019) observed meltwater-induced phytoplankton production in the marginal ice zone near Fram Strait in May 2019, which continued until the end of August. Photosynthesis in the upper few meters of the water column could reduce fCO_{2w}.

Air-sea gas exchange cannot be the cause of the lower surface fCO_{2w} observed in stratified waters because the influx of CO_2 would have not help to explain the observations, increasing fCO_{2w} at the surface. The results presented here demonstrate that near-surface stratification due to sea-ice melt generates a strong near-surface fCO_{2w} gradient ($fCO_{2w\_surface} < fCO_{2w\_bulk}$), which causes a bias in bulk air-sea CO_2 flux estimates when fCO_{2w_bulk} from ~6 m depth is used. In the next section, we estimate the impact of such a bias would have on CO_2 uptake by the entire Arctic Ocean.

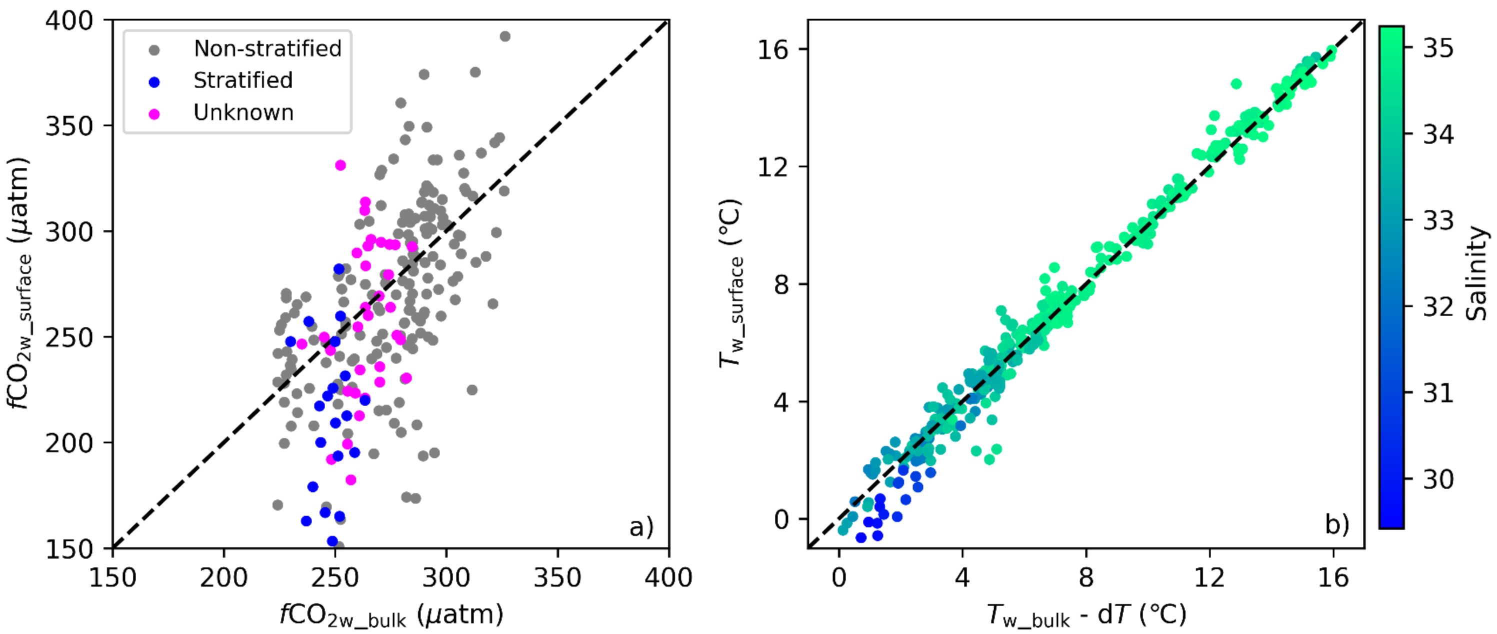

Figure 3. Measurements at 6 m depth of seawater CO_2 fugacity (fCO_{2w_bulk}) and temperature (corrected for the cool skin effect, i.e. $T_{w\_bulk} - dT$) versus eddy covariance implied sea surface CO_2 fugacity ($fCO_{2w\_surface}$) and temperature ($T_{w\_surface}$): a) fCO_2 values from cruise JR18007. Grey dots are values in non-stratified waters, blue dots are in stratified waters and magenta dots are in waters for which the

stratification status could not be determined; b) Seawater temperature for JR18006 and JR18007 with the dots colour-coded by salinity at 6 m depth.

3.4 Potential Impact on Arctic Ocean CO_2 Uptake Estimates

Here we speculate on the potential impact of near-surface stratification due to summertime sea-ice melt on estimates of CO_2 uptake for the entire Arctic Ocean.

We make the following crude assumptions: 1) bulk fCO_{2w} measurements overestimate the surface fCO_{2w} in all regions with sea-ice melt; 2) the fCO_{2w} overestimation (-fCO_{2w} offset, µatm) decreases with wind speed for $U_{10N} > 3$ m s^{-1} ($f\mathrm{CO_{2w}}$ offset $= -408\ U_{10N}^{-1} + 27$, Figure S5) (Fischer et al., 2019; Miller et al., 2019; Ahmed et al., 2020) and is assumed to be constant (109 µatm) at $U_{10N} \leq 3$ m s^{-1}; 3) surface seawater temperature and salinity are 2°C and 31 within the stratified areas, respectively (average of the EC implied $T_{w\_surface}$ and surface salinity in the stratified waters during JR18007).

The 6-hour Cross-Calibrated Multi-Platform (CCMP) Wind Vector Analysis (Atlas et al., 2011) at a height of 10 m above mean sea level is used to calculate K_{660} and to estimate the fCO_{2w} offset. The flux offset is calculated with Equation 1 (replacing ΔfCO_2 with fCO_{2w} offset), and the result from each grid cell is linearly scaled using the sea ice concentration. The AMSR-E (Spreen et al., 2008) daily sea ice concentration (SIC) data (3.125 km grid resolution) are used to determine the extent of stratified areas. There are two scenarios when a grid cell is deemed to contain near-surface stratified water: 1) the ice-free proportion of the grid cell is considered to be stratified when SIC is between 0% and 100%; 2) SIC of a grid cell has declined to 0% during the last 10 days (assuming that near-surface stratification lasts for 10 days, within the indicated duration time indicated by Ahmed et al., 2020), the whole cell is considered to be stratified.

We focus on the summertime (June to August inclusive) Arctic Ocean in 2019. The result shows that the largest area with near-surface stratification and the greatest underestimation of CO_2 uptake occur in July (Figure S6). K_{660} increases with the wind speed, while the magnitude of fCO_{2w} offset decreases with wind speed, so the wind speed effect on the variability of the flux offset is almost cancelled out and the estimated bulk flux variability is mainly related to the size of the stratified area. The integrated summertime underestimation of Arctic Ocean CO_2

uptake due to sea-ice melt is estimated to be 11 Tg C, which is comparable with the back-of-the-envelope calculation (9.3 Tg C yr^{-1}) of Ahmed et al. (2020)

The above estimate is based on assumptions that the fCO_{2w} offset is wind speed dependent and the shallow stratification lasts for 10 days. High wind speed enhances the near-surface seawater mixing and weakens the shallow stratification. We do not have a robust relationship between fCO_{2w} offset and wind speed because our measurements in stratified waters only span a small range of wind speeds (6 ± 1 m s^{-1}) and the data are quite scattered (Figure S5). If we do not consider the influence of wind speed on the fCO_{2w} gradient and assume a constant fCO_{2w} offset of -39 µatm in the sea ice melt region, then the underestimation of Arctic Ocean CO_2 uptake is reduced to 6 Tg C. Another major uncertainty is inherent in our assumption that near-surface stratification lasts for 10 days. If we assume that the near-surface stratification lasts 7 days or 14 days, the underestimation of Arctic Ocean CO_2 uptake is 10 Tg C and 13 Tg C, respectively (using the wind speed dependent fCO_{2w} offset).

The underestimation of 11 Tg C in 2019 corresponds to 6–17% of annual Arctic Ocean carbon uptake (66–199 Tg C yr^{-1}, Bates & Mathis, 2009). Note that the CO_2 sink estimate by Bates & Mathis (2009) was a decade ago, so the percentage of this underestimate may have slightly changed.

4. Conclusions

This study reports direct and indirect estimates of air-sea CO_2 and sensible heat fluxes from shipboard campaigns in the summertime Arctic Ocean. Direct fluxes by eddy covariance are used to compute the implied sea surface fCO_{2w} and T_w . Comparisons of implied surface values with bulk water measurements at 6 m depth help to identify possible vertical fCO_{2w} gradients in the upper ocean. Implied surface fCO_{2w} is on average 39 µatm lower than bulk fCO_{2w} in regions with near-surface stratification due to sea ice melt. EC-derived gas transfer velocities (K_{660}) using bulk seawater measurements in non-stratified regions agree well with previous parameterizations. However, in stratified regions, EC-derived K_{660} is higher at a given wind speed because of the near-surface fCO_{2w} gradient.

Cooling and freshening due to sea-ice melt in the Arctic summer accounts for 18% and at least 27% of the near-surface fCO_{2w} gradient during cruise JR18007, respectively. Enhanced photosynthesis in the stratified layer may also have contributed to the near-surface fCO_{2w} gradient.

The Arctic Ocean is an important CO_2 sink, but this ocean carbon uptake may have been underestimated previously due to near-surface fCO_{2w} gradients induced by sea-ice melt. A simple calculation for the summertime Arctic Ocean suggests that near-surface stratification due to sea-ice melt could lead to an ~10 Tg C underestimation of CO_2 uptake but there is considerable uncertainty in the validity of such an extrapolation. Continuing loss of Arctic sea ice is expected to increase CO_2 uptake in summer, and may further increase the uncertainty in Arctic air-sea CO_2 flux estimates if near-surface stratification is not considered.

This is the first time to our knowledge that direct measurements by EC have been used to quantify the potential bias in bulk flux estimates due to near-surface stratification in the Arctic Ocean. A similar underestimation in CO_2 flux related to sea-ice melt may also occur in the Southern Ocean. Detailed studies of upper ocean (0–10 m) gradients in fCO_{2w}, temperature, salinity, DIC, TA and biological rates along with EC flux measurements, are required to improve understanding of sea-ice melt impacts and near-surface stratification on air-sea exchange.

Data Availability Statement. The raw EC data and hourly flux data can be accessed at: https://doi.org/10.5285/03C78C45-08B5-4D82-B09D-09C0B8A32C4D. The CTD profile data are stored at the British Oceanographic Data Centre (BODC): https://www.bodc.ac.uk/data/bodc_database/nodb/cruise/17335/. AMSR-E data: https://seaice.uni-bremen.de/data/amsr2/asi_daygrid_swath/n3125/. CCMP data: http://data.remss.com/ccmp/v02.1.NRT/

Acknowledgements: The Natural Environment Research Council (NERC) supported the Arctic research campaigns (DIAPOD, NE/P006280/2; ChAOS, NE/P006493/1 and PETRA, NE/R012830/1). CO_2 flux measurements were made possible by funding from the NERC ORCHESTRA (NE/N018095/1) and European Space Agency AMT4oceanSatFluxCCN (4000125730/18/NL/FF/gp) projects. DIC/TA data were supported by Flagship program "Ocean Acidification and effects in northern waters" within the FRAM-High North Research Centre for Climate and Environment, Tromsø, Norway. We thank captains and crew of RRS *James Clark Ross* and all those who helped keep the CO_2 flux system running. We thank Robyn Owen (BODC) for her kind help with the CTD profile data. The analysis of these data is supported by the China Scholarship Council (CSC/201906330072).

References

Ahmed, M. M. M., Else, B. G. T., Capelle, D., Miller, L. A., & Papakyriakou, T. (2020). Underestimation of surface pCO_2 and air-sea CO_2 fluxes due to freshwater stratification in an Arctic shelf sea, Hudson Bay. *Elementa: Science of the Anthropocene*, 8(1): 084. https://doi.org/10.1525/elementa.084

Anderson, L. G., Olsson, K., & Chierici, M. (1998). A carbon budget for the Arctic Ocean. *Global Biogeochemical Cycles*, *12*(3), 455–465. https://doi.org/10.1029/98GB01372

Arrigo, K. R., & van Dijken, G. L. (2015). Continued increases in Arctic Ocean primary production. Progress in Oceanography, 136, 60–70. https://doi.org/10.1016/j.pocean.2015.05.002

Assmy, P., Fernández-Méndez, M., Duarte, P., Meyer, A., Randelhoff, A., Mundy, C. J., et al. (2017). Leads in Arctic pack ice enable early phytoplankton blooms below snow-covered sea ice. *Scientific Reports*, *7* (40850 2017), 1–9. https://doi.org/10.1038/srep40850

Atlas, R., Hoffman, R. N., Ardizzone, J., Leidner, S. M., Jusem, J. C., Smith, D. K., & Gombos, D. (2011). A cross-calibrated, multiplatform ocean surface wind velocity product for meteorological and oceanographic applications. *Bulletin of the American Meteorological Society*, *92*(2), 157–174. https://doi.org/10.1175/2010BAMS2946.1

Bates, N. R., & Mathis, J. T. (2009). The Arctic Ocean marine carbon cycle: evaluation of air-sea CO_2 exchanges, ocean acidification impacts and potential feedbacks. *Biogeosciences*, *6*(11). https://doi.org/10.5194/bg-6-2433-2009, 2009

Butterworth, B. J., & Miller, S. D. (2016). Air-sea exchange of carbon dioxide in the Southern Ocean and Antarctic marginal ice zone. *Geophysical Research Letters*, *43*(13), 7223–7230. https://doi.org/10.1002/2016GL069581

Butterworth, B. J., & Else, B. G. T. (2018). Dried, closed-path eddy covariance method for measuring carbon dioxide flux over sea ice. *Atmospheric Measurement Techniques*, *11*(11), 6075–6090. https://doi.org/10.5194/amt-11-6075-2018

Cai, W.-J., Chen, L., Chen, B., Gao, Z., Lee, S. H., Chen, J., et al. (2010). Decrease in the CO_2 uptake capacity in an ice-free Arctic Ocean basin. *Science*, *329*(5991), 556–559. https://doi.org/10.1126/science.1189338

Calleja, Maria Ll, Duarte, C. M., Álvarez, M., Vaquer-Sunyer, R., Agustí, S., & Herndl, G. J. (2013). Prevalence of strong vertical CO_2 and O_2 variability in the top meters of the ocean. *Global Biogeochemical Cycles*, *27*(3), 941–949. https://doi.org/10.1002/gbc.20081

Chierici, M., Vernet, M., Fransson, A., & Børsheim, K. Y. (2019). Net community production and carbon exchange from winter to summer in the Atlantic water inflow to the Arctic Ocean. *Frontiers in Marine Science*, *6*(September), 1–24. https://doi.org/10.3389/fmars.2019.00528

Dong, Y., Yang, M., Bakker, D. C. E., Kitidis, V., & Bell, T. G. (2021). Uncertainties in eddy covariance air-sea CO_2 flux measurements and implications for gas transfer velocity parameterisations. *Atmospheric Chemistry and Physics*, *21*(10), 8089–8110. https://doi.org/10.5194/acp-21-8089-2021

Edson, J. B, Jampana, V., Weller, R. A., Bigorre, S. P., Plueddemann, A. J., Fairall, C. W., et al. (2013). On the exchange of momentum over the open ocean. *Journal of Physical Oceanography*, *43*(8), 1589–1610. https://doi.org/10.1175/JPO-D-12-0173.1

Else, Brent G T, Galley, R. J., Lansard, B., Barber, D. G., Brown, K., Miller, L. A., et al. (2013). Further observations of a decreasing atmospheric CO_2 uptake capacity in the Canada Basin (Arctic Ocean) due to sea ice loss. *Geophysical Research Letters*, *40*(6), 1132–1137. https://doi.org/10.1002/grl.50268

Fairall, C. W., Bradley, E. F., Godfrey, J. S., Wick, G. A., Edson, J. B., & Young, G. S. (1996). Cool-skin and warm-layer effects on sea surface temperature. *Journal of Geophysical Research: Oceans*, *101*(C1), 1295–1308. https://doi.org/10.1029/95JC03190

Fischer, T., Kock, A., Arévalo-Martínez, D. L., Dengler, M., Brandt, P., & Bange, H. W. (2019). Gas exchange estimates in the Peruvian upwelling regime biased by multi-day near-surface stratification. *Biogeosciences*, *16*(11), 2307–2328. https://doi.org/10.5194/bg-16-2307-2019

Fransson, A., Chierici, M., & Nojiri, Y. (2009). New insights into the spatial variability of the surface water carbon dioxide in varying sea ice conditions in the Arctic Ocean. *Continental Shelf Research*, *29*(10), 1317–1328. https://doi.org/10.1016/j.csr.2009.03.008

Fransson, A., Chierici, M., Miller, L. A., Carnat, G., Shadwick, E., Thomas, H., et al. (2013). Impact of sea-ice processes on the carbonate system and ocean acidification at the ice-water interface of the Amundsen Gulf, Arctic Ocean. *Journal of Geophysical Research: Oceans*, *118*(12), 7001–7023. https://doi.org/10.1002/2013JC009164

Fransson, A., Chierici, M., Skjelvan, I., Olsen, A., Assmy, P., Peterson, A. K., et al. (2017). Effects of sea-ice and biogeochemical processes and storms on under-ice water fCO_2 during the winter-spring transition in the high Arctic Ocean: Implications for sea-air CO_2 fluxes. *Journal of Geophysical Research: Oceans, 122*(7), 5566–5587. https://doi.org/https://doi.org/10.1002/2016JC012478

Van Heuven, S., Pierrot, D., Rae, J. W. B., Lewis, E., & Wallace, D. W. R. (2011). MATLAB program developed for CO_2 system calculations. *ORNL/CDIAC-105b*, *530*.

Jähne, B. (2009). Air–sea gas exchange. in *Encyclopedia Ocean Sciences, edited by J. H. Steele, K. K. Turekian, and S. A. Thorpe, pp. 3434–3444, Elsevier, San Diego, Calif.*

Landschützer, P., Gruber, N., Bakker, D. C. E., & Schuster, U. (2014). Recent variability of the global ocean carbon sink. Global Biogeochemical Cycles, 28(9), 927–949. https://doi.org/10.1002/2014GB004853

Landwehr, S., O'Sullivan, N., & Ward, B. (2015). Direct flux measurements from mobile platforms at sea: Motion and airflow distortion corrections revisited. *Journal of Atmospheric and Oceanic Technology*, *32*(6), 1163–1178. https://doi.org/10.1175/JTECH-D-14-00137.1

Lewis, E. R., & Wallace, D. W. R. (1998). *Program developed for CO_2 system calculations*. Environmental System Science Data Infrastructure for a Virtual Ecosystem. https://doi.org/10.15485/1464255

Li, W. K. W., McLaughlin, F. A., Lovejoy, C., & Carmack, E. C. (2009). Smallest algae thrive as the Arctic Ocean freshens. *Science*, *326*(5952), 539. https://doi.org/10.1126/science.1179798

Liss, P. S., & Slater, P. G. (1974). Flux of gases across the air-sea interface. *Nature*, *247*(5438), 181–184. https://doi.org/10.1038/247181a0

Loose, B., Miller, L. A., Elliott, S., & Papakyriakou, T. (2011). Sea ice biogeochemistry and material transport across the frozen interface. *Oceanography*, *24*(3), 202–218. https://doi.org/10.5670/oceanog.2011.72

McPhee, M. G., Proshutinsky, A., Morison, J. H., Steele, M., & Alkire, M. B. (2009). Rapid change in freshwater content of the Arctic Ocean. Geophysical Research Letters, 36(10). https://doi.org/10.1029/2009GL037525

Miller, L. A., Burgers, T. M., Burt, W. J., Granskog, M. A., & Papakyriakou, T. N. (2019). Air-sea CO_2 flux estimates in stratified arctic coastal waters: how wrong can we be? *Geophysical Research Letters*, *46*(1), 235–243. https://doi.org/10.1029/2018GL080099

Nightingale, P. D., Malin, G., Law, C. S., Watson, A. J., Liss, P. S., Liddicoat, M. I., et al. (2000). In situ evaluation of air-sea gas exchange parameterizations using novel conservative and volatile tracers. *Global Biogeochemical Cycles*, *14*(1), 373–387. https://doi.org/10.1029/1999GB900091

Perovich, D. K., Light, B., Eicken, H., Jones, K. F., Runciman, K., & Nghiem, S. V. (2007). Increasing solar heating of the Arctic Ocean and adjacent seas, 1979–2005: Attribution and role in the ice-albedo feedback. *Geophysical Research Letters*, *34*(19), L19505. https://doi.org/10.1029/2007GL031480

Perovich, D., Meier, W., Tschudi, M., Hendricks, S., Petty, A. A., Divine, D., et al. (2020). Arctic

Report Card 2020: Sea Ice. (U. S. N. O. and A. A. O. of O. and A. R. P. M. E. L. (U.S.), T. S. of Engineering, N. S. and I. D. C. (U.S.), U. of C. (Boulder campus), H. C. for P. and M. R. Alfred-Wegener-Institut für Polar- und Meeresforschung / Alfred Wegener Institute, G. S. F. Center, et al., Eds.). https://doi.org/https://doi.org/10.25923/n170-9h57

Prytherch, John, Brooks, I. M., Crill, P. M., Thornton, B. F., Salisbury, D. J., Tjernström, M., et al. (2017). Direct determination of the air-sea CO_2 gas transfer velocity in Arctic sea ice regions. *Geophysical Research Letters*, *44*(8), 3770–3778. https://doi.org/10.1002/2017GL073593

Prytherch, J., & Yelland, M. J. (2021). Wind, convection and fetch dependence of gas transfer velocity in an Arctic sea-ice lead determined from eddy covariance CO_2 flux measurements. *Global Biogeochemical Cycles*, *35*, e2020GB006633. https://doi.org/10.1029/2020GB006633

Romanovsky, V., Isaksen, K., D, D., Anisimov, O., A, I., Leibman, M., et al. (2017). Changing permafrost and its impacts. In: Snow, Water, Ice and Permafrost in the Arctic (SWIPA) 2017 (pp. 65–102). http://hdl.handle.net/11374/1931

Rudels, B., Björk, G., Nilsson, J., Winsor, P., Lake, I., & Nohr, C. (2005). The interaction between waters from the Arctic Ocean and the Nordic Seas north of Fram Strait and along the East Greenland Current: Results from the Arctic Ocean-02 Oden expedition. *Journal of Marine Systems*, *55*(1–2), 1–30. https://doi.org/10.1016/j.jmarsys.2004.06.008

Rysgaard, S., Glud, R. N., Sejr, M. K., Bendtsen, J., & Christensen, P. B. (2007). Inorganic carbon transport during sea ice growth and decay: A carbon pump in polar seas. *Journal of Geophysical Research: Oceans*, *112*(3), 1–8. https://doi.org/10.1029/2006JC003572

Spreen, G., Kaleschke, L., & Heygster, G. (2008). Sea ice remote sensing using AMSR-E 89-GHz channels. *Journal of Geophysical Research: Oceans*, *113*(C2). https://doi.org/10.1029/2005JC003384

Takahashi, T., Olafsson, J., Goddard, J. G., Chipman, D. W., & Sutherland, S. C. (1993). Seasonal variation of CO_2 and nutrients in the high-latitude surface oceans: A comparative study. *Global Biogeochemical Cycles*, *7*(4), 843–878. https://doi.org/10.1029/93GB02263

Takahashi, T., Sutherland, S. C., Wanninkhof, R., Sweeney, C., Feely, R. A., Chipman, D. W., et al. (2009). Climatological mean and decadal change in surface ocean *p*CO2, and net sea-air CO_2 flux over the global oceans. *Deep Sea Research Part II: Topical Studies in Oceanography*, *56*(8–10), 554–577. https://doi.org/10.1016/J.DSR2.2008.12.009

Wanninkhof, R., Asher, W. E., Ho, D. T., Sweeney, C., & McGillis, W. R. (2009). Advances in quantifying air-sea gas exchange and environmental forcing. *Annual Review of Marine Science*, *1*(1), 213–244. https://doi.org/10.1146/annurev.marine.010908.163742

Weiss, R. F. (1974). Carbon dioxide in water and seawater: the solubility of a non-ideal gas. *Marine Chemistry*, *2*(3), 203–215. https://doi.org/10.1016/0304-4203(74)90015-2

Woolf, D. K., Land, P. E., Shutler, J. D., Goddijn-Murphy, L. M., & Donlon, C. J. (2016). On the calculation of air-sea fluxes of CO_2 in the presence of temperature and salinity gradients. *Journal of Geophysical Research: Oceans*, *121*(2), 1229–1248. https://doi.org/10.1002/2015JC011427

Yamamoto-Kawai, M., McLaughlin, F. A., Carmack, E. C., Nishino, S., & Shimada, K. (2009). Aragonite undersaturation in the Arctic Ocean: effects of ocean acidification and sea ice melt. *Science*, *326*(5956), 1098–1100. https://doi.org/10.1126/science.1174190

Yang, M., Bell, T. G., Blomquist, B. W., Fairall, C. W., Brooks, I. M., & Nightingale, P. D. (2016). Air-sea transfer of gas phase controlled compounds. In *IOP Conference Series: Earth and Environmental Science* (Vol. 35, p. 12011). IOP Publishing. https://doi.org/10.1088/1755-1315/35/1/012011

Yasunaka, S., Siswanto, E., Olsen, A., Hoppema, M., Watanabe, E., Fransson, A., et al. (2018). Arctic Ocean CO_2 uptake: an improved multiyear estimate of the air–sea CO_2 flux incorporating chlorophyll a concentrations. *Biogeosciences*, *15*(6), 1643–1661. https://doi.org/10.5194/bg-15-1643-2018, 2018

References From the Supporting Information

Dong, Y., Yang, M., Bakker, D. C. E., Kitidis, V., & Bell, T. G. (2021). Uncertainties in eddy covariance air–sea CO_2 flux measurements and implications for gas transfer velocity parameterisations. *Atmospheric Chemistry and Physics*, *21*(10), 8089–8110. https://doi.org/10.5194/acp-21-8089-2021

Donlon, C. J., Minnett, P. J., Gentemann, C., Nightingale, T. J., Barton, I. J., Ward, B., & Murray, M. J. (2002). Toward improved validation of satellite sea surface skin temperature measurements for climate research. *Journal of Climate*, *15*(4), 353–369. https://doi.org/10.1175/1520-0442(2002)015<0353:TIVOSS>2.0.CO;2

Edson, J. B., Hinton, A. A., Prada, K. E., Hare, J. E., & Fairall, C. W. (1998). Direct covariance flux estimates from mobile platforms at sea. *Journal of Atmospheric and Oceanic Technology*, *15*(2), 547–562. https://doi.org/10.1175/1520-0426(1998)015<0547:DCFEFM>2.0.CO;2

Edson, J. B, Jampana, V., Weller, R. A., Bigorre, S. P., Plueddemann, A. J., Fairall, C. W., et al. (2013). On the exchange of momentum over the open ocean. *Journal of Physical Oceanography*, *43*(8), 1589–1610. https://doi.org/10.1175/JPO-D-12-0173.1

Fairall, C. W., Bradley, E. F., Godfrey, J. S., Wick, G. A., Edson, J. B., & Young, G. S. (1996). Cool-skin and warm-layer effects on sea surface temperature. *Journal of Geophysical Research: Oceans*, *101*(C1), 1295–1308. https://doi.org/10.1029/95JC03190

Kitidis, V., Brown, I., Hardman-Mountford, N., & Lefèvre, N. (2017). Surface ocean carbon dioxide during the Atlantic Meridional Transect (1995–2013); evidence of ocean acidification. *Progress in Oceanography*, *158*, 65–75. https://doi.org/10.1016/j.pocean.2016.08.005

Nightingale, P. D., Malin, G., Law, C. S., Watson, A. J., Liss, P. S., Liddicoat, M. I., et al. (2000). In situ evaluation of air-sea gas exchange parameterizations using novel conservative and volatile tracers. *Global Biogeochemical Cycles*, *14*(1), 373–387. https://doi.org/10.1029/1999GB900091

Spreen, G., Kaleschke, L., & Heygster, G. (2008). Sea ice remote sensing using AMSR-E 89-GHz channels. *Journal of Geophysical Research: Oceans*, *113*(C2). https://doi.org/10.1029/2005JC003384

Takahashi, T., Olafsson, J., Goddard, J. G., Chipman, D. W., & Sutherland, S. C. (1993). Seasonal variation of CO_2 and nutrients in the high-latitude surface oceans: A comparative study. *Global Biogeochemical Cycles*, *7*(4), 843–878. https://doi.org/10.1029/93GB02263

Yang, M., Bell, T. G., Blomquist, B. W., Fairall, C. W., Brooks, I. M., & Nightingale, P. D. (2016). Air-sea transfer of gas phase controlled compounds. In *IOP Conference Series: Earth and Environmental Science* (Vol. 35, p. 12011). IOP Publishing. https://doi.org/10.1088/1755-1315/35/1/012011